Model of different nucleation rates within particular zones of the area of polycrystalline platinum electrode for describing the initial stages of deposition of bismuth from perchlorate solution

Vidmantas Kapočius, Laima Gudavičiūtė, Violeta Karpavičienė and Antanas Steponavičius

Institute of Chemistry,
A. Goštauto 9,
LT-2600, Vilnius, Lithuania

The initial stages of Bi deposition onto smooth polycrystalline Pt electrode from acidic 0.1 M Bi^{3+} perchlorate solution at 20 °C were investigated using a potential step technique. On the basis of analysis of the current transients, it has been shown that the initial stages of Bi electrocrystallization onto Pt quite well fit the progressive 3D nucleation and diffusion-controlled growth mechanism by Scharifker and Hills, taking into account the presence of the separate zones with different metal nucleation rates on the electrode surface. It was also assumed that these separate zones should be of macroscopic dimensions rather than microscopic or atomic ones.

Key words: bismuth, deposition, initial stages, polycrystalline platinum, perchlorate solution

INTRODUCTION

The initial stages of electrodeposition of metal (*M*) on a foreign substrate (*S*) are of practical importance in various fields of modern technology, *e.g.* in producing materials for electrocatalysis, microelectronics, magnetic devices, etc. Investigations of the *M* ions adsorption reactions and 2D and 3D nucleation and growth processes, which play a crucial role in electrochemical phase formation, have been reviewed recently (see, *e.g.*, [1–4]). Three types of growth modes were distinguished, depending on the binding energies of *M* adatoms on a foreign and on the same *S* and the crystallographic *M*–*S* misfit (these typical modes are known as Frank–Van der Merwe, Stranski–Krastanov and Volmer–Weber mechanisms [1]). Mathematical description of 3D nucleation / growth processes in the overpotential range for different models was presented in detail in a number of papers [5–16]. The morphological and energetic state of *S* surface was pointed out to be an important problem connected with the electrochemical new phase formation [17, 18]. Besides, the underpotential phenomena, which are frequently observed, can complicate additionally the examination of the nucleation process because in that case an original *S* surface becomes rather masked [17, 18].

Among metals which have considerable promises for the modern technology, bismuth seems to be worth mentioning [19–21]. Bi in a submonolayer range on various *S* was proposed to be used widely for electrocatalysis in numerous redox reactions. Thin films of this metal have technological application in wide-range field and current sensors, owing to Bi unusual electronic properties. Although the underpotential deposition (UPD) of Bi onto various *S* is well documented in a number of papers [22–39], to our knowledge, there are actually no investigations of early stages of Bi electrodeposition onto a foreign *S*.

The preliminary results on this subject have been presented recently in our study [40]. In particular, analysing the experimental chronoamperometric data within the framework of the theory of Scharifker and Hills [10], it was found that the initial stages of Bi deposition on a smooth polycrystalline Pt electrode from acidic perchlorate solutions quite well fitted the progressive 3D nucleation and growth under diffusion control model. Some nucleation parameters were also evaluated, depending on the experimental conditions. However, predictions derived from the theory [10] were satisfied not in all cases. For example, it was found that the conventional treatment of the current transients led to a significantly lower value of the diffusion coefficient of Bi^{3+} ion [40]. Besides, under certain conditions of electrolysis, two waves in the current–time curves were ob-

served. These findings were not sufficiently explained in the cited work.

The aim of the present work was to investigate the initial stages of Bi electrodeposition onto a smooth polycrystalline Pt electrode from acidic perchlorate solution. With this purpose in mind, attempts were also made to interpret the features of the current transients mentioned above, which until now remained little understood.

EXPERIMENTAL

The chronoamperometric experiments were carried out in 1 M $HClO_4$ + 0.1 M $Bi(ClO_4)_3$ solution prepared from chemicals of the highest purity and triply-distilled water. The electrolyte was deaerated prior to each experiment by bubbling purified argon for 1 h.

Chronoamperometric studies were performed in a conventional three-electrode cell. The working electrode was a vertical disc made from a mat polycrystalline Pt foil (99.99% purity) and sealed into a soft glass tube. The geometric area of the working electrode was 1 cm^2. Its real area was determined from a hydrogen adsorption voltammetric profile recorded at 50 mV s^{-1} in 0.5 M H_2SO_4 solution, taking the theoretical hydrogen adsorption charge of 210 μC cm^{-2}, as noted in [41]. The roughness factor (f) was found to be equal to 2.0 ± 0.1. The counter-electrode was a Pt sheet of ca. 6 cm^2 in area. The reference electrode was an Ag/AgCl/KCl(sat.) electrode provided with a KNO_3 salt bridge in order to avoid contamination of the working solution with Cl^- ions. All potentials (E) in the text are referred to the SHE scale. Unless otherwise noted, all currents (i) are reported with respect to the geometric area of the Pt working electrode.

All glassware was cleaned before use with warm concentrated H_2SO_4 for 2 h, rinsed with doubly-distilled water and left in it overnight.

The working electrode was subjected to an initial pretreatment as follows: (*i*) slight mechanical polishing with diamond paste down to 0.1 μm; (*ii*) immersion in chromic acid for 4 h at ambient temperature followed by immersion in 0.5 M H_2SO_4 for 24 h and thorough rinsing with doubly-distilled water; (*iii*) electrochemical activation by repetitive triangular cycling between +0.05 and +1.30 V in 0.5 M H_2SO_4 solution at 50 mV s^{-1} for 15 h (a volume of solution was changed several times). Before each experiment, the pretreatment involved such stages: (*i*) immersion in chromic acid for 10 min followed by immersion in 0.5 M H_2SO_4 solution for 0.5 h and electrochemical activation by repetitive cycling in 0.5 M H_2SO_4 solution at 50 mV s^{-1} between +0.05 and +1.30 V until a stationary voltammogram characteristic of polycrystalline Pt [42, 43] was observed (the potential scan was stopped during the cathodic half-cycle at E = +0.40 V); (*ii*) finally, transfer of the electrode to the another cell with the working solution under a drop of electrolyte.

The experimental procedure was as follows: (*i*) after contacting with the working solution, the working electrode was held for 5 min at the starting potential E_{start} = +0.3 V being in the UPD range; (*ii*) then, E was stepped to the selected deposition potentials E_{dep} in the OPD zone for the deposition time t_{dep} = 40 s; (*iii*) after disconnecting the electronic circuit of the potentiostat, the bismuth-covered Pt electrode was left in the working solution until its E approached spontaneously the value of ca. +0.8 V; (*iv*) the remaining amount of Bi deposit was desorbed oxidatively by polarization at +1.30 V for 1 min, followed by immersion in nitric acid (1:1) for 5 min and rinsing with doubly-distilled water; (*v*) the working electrode was then transferred to the cell with 0.5 M H_2SO_4 solution to be subjected to repetitive cycling at 50 mV s^{-1} between +0.02 and +1.30 V until the i/E profile characteristic of the clean Pt electrode [42, 43] was again recorded. Each single-step potentiostatic experiment was preceded by such a pretreatment of the working electrode.

The chronoamperometric measurements were carried out at a temperature of 20 °C, using a PI 50–1 potenciostat (made in Belorus) interfaced through a home-made analogue to digital converter with a PC (Siemens) and a PR-8 programmer (made in Belarus). The experimental data acquisition was in a numerical form with a time resolution of 4 or 50 ms per point.

RESULTS AND DISCUSSION

The nucleation process was analyzed using the single potential step technique. Figure 1 shows a family of typical current transients obtained at different E pulses. In most cases, the shape of the transients can be formally explained on the basis of the theory of 3D nucleation with diffusion-controlled growth [10], *i.e.* a rising current in the initial part of the transient showing an increase in the deposit formation rate to a certain maximum is followed by an asymptotically descending part before the curves merge into one. In some instances, the shape of the current transients, however, departs from that predicted by the theory [10]. In particular, a second increase in current in the range of longer times can be observed in the transients (Fig. 1, curve 2). Such an observation appears to be not reported in the available literature, but some information on this point was presented in our previous work [40].

Assuming that for Bi, as for most metals, the charge transfer rate is sufficiently high and the con-

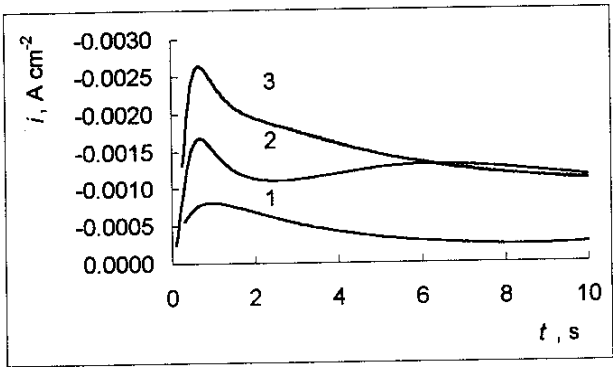

Fig. 1. Typical potentiostatic current transients for the electrodeposition of Bi onto smooth polycrystalline Pt from 0.1 M Bi^{3+} perchlorate solution at overpotentials: *1* – 49 mV, *2* – 53 mV and *3* – 57 mV. $E_{eq.}$ = +0.238 V, $E_{start.}$ = +0.30 V, temperature 20 °C

tinued growth of formed nuclei is entirely mass-transfer-controlled, two limiting cases of multiple nucleation with diffusion-controlled growth can be conventionally considered depending on the nucleation rate, in accordance with the theory [10].

In the first case, at high nucleation rates, all nuclei are formed immediately after the potential step and their number remains constant during the growth process. This case is considered as instantaneous nucleation and is described by [10]:

$$i(t) = [zFD^{0.5}c/(\pi t)^{0.5}]\ [1\text{-}\exp(-N\pi kDt)], \qquad (1)$$

where $i(t)$ is current density related to the geometric area of the electrode surface, N the total number of the formed nuclei, k the numerical constant calculated from [10]:

$$k = (8\pi cM/\rho)^{0.5}, \qquad (2)$$

M and ρ are the molar mass and the density of deposited metal, zF the molar charge of the electrodepositing species, D the diffusion coefficient, c the bulk concentration (in mol cm^{-3}).

The second case, at small nucleation rates, when the nuclei are continuously formed during the whole time window before overlapping of diffusion hemispheres around the growing nuclei, is called progressive nucleation [10]. In this case, the metal clusters of different sizes can be formed, especially at the very initial t. The current transients for the progressive 3D nucleation-growth mechanism are given by [10]:

$$i(t) = [zFD^{0.5}c/(\pi t)^{0.5}]\ [1\text{-}\exp\ (-aN_0\,\pi\,k'Dt^2/2], \qquad (3)$$

where N_0 is the number density of substrate active sites, a is the steady-state nucleation rate constant per site, k' is again a numerical constant given by [10]:

$$k' = (4/3)\ (8\pi cM/\rho)^{0.5}. \qquad (4)$$

In order to characterize the nucleation process, the current transients can be plotted in reduced valuables $(i/i_{max})^2$ vs. t/t_{max} [10]. Figure 2 shows such a presentation of the $(i/i_{max})^2$ *vs.* t/t_{max} plots calculated from the relations [10] – for instantaneous nucleation:

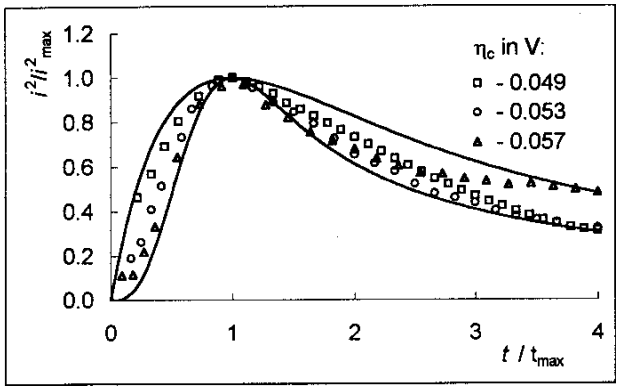

Fig. 2. Non-dimensional $(i/i_{max})^2$ *vs.* t/t_{max} plots. Calculated curves: for instantaneous 3D nucleation and diffusion-controlled growth model [10] (curve 1) and for progressive one [10] (curve 2). Experimental data are given as respective points

$$(i/i_{max})^2 = 1.9542\ (t/t_{max})^{-1}\ \{1\text{–}\exp[\text{–}1.2564\ (t/t_{max})]\}^2 \qquad (5)$$

and for progressive nucleation:

$$(i/i_{max})^2 = 1.2254\ (t/t_{max})^{-1}\ \{1\text{–}\exp[\text{–}2.3367\ (t/t_{max})^2]\}^2 \qquad (6)$$

together with the experimental data obtained in the present work. Although there is a certain scattering of the experimental points, it seems that the experimental data fit rather well those calculated for the progressive nucleation mechanism. Therefore, the Bi electrodeposition onto smooth polycrystalline Pt is assumed to be described by a model involving progressive 3D nucleation and diffusion-controlled growth.

On the other hand, it is important to note that this assumption strongly needs to be complemented, because some characteristics of the transients recorded here do not satisfy the theory [10] requirements. The occurrence of the second increase in current at longer times in the transients (Fig. 1) should be mentioned first. Further, the values of product aN_o, *i.e.* the nucleation rate calculated from the expressions for t_{max} and i_{max} for progressive nucleation [10]

$$t_{max} = (4.6733 / aN_o \pi k'D)^{0.5}, \quad (7)$$

$$i_{max} = 0.4615\ zFD^{3/4}(k'aN_o)^{1/4} \quad (8)$$

were obtained to be different. Besides, although the calculated value of product $i^2_{max}\ t_{max}$ is independent of η_c applied, as is evident from expression [10]

$$i^2_{max} \cdot t_{max} = 0.2598\ (zFc)^2D, \quad (9)$$

it was obtained that this product varied rather indefinitely with η_c and its average value gave D being about two orders of magnitude less than the value characteristic of the diffusion of ions in aqueous solutions (in this paper overpotentials η_c were referred to the equilibrium potential E_{eq} of the couple Bi/Bi^{3+} which was found to be equal +0.238 V).

Our starting point for the interpretation of the observed features of the experimental current transients will be a concept of inhomogeneity of an inert S surface as to a nucleation rate aN_o being different in different zones of the S surface due to a certain accumulation of surface crystallographic defects in these zones, while the rest of surface is likely characterized by a rather random distribution of the defects.

It will be recalled that the impact of the state of various S in electrochemical nucleation has been already studied in a number of papers, mainly with regard to an agreement of the number density of actives sites (N_o) on the foreign S surface with the maximal number of nuclei which can be formed at given experimental conditions (see, e.g. [11, 12]), or to the nucleation rate as a phenomenon in which nucleation occurs at different rates at different active sites on the S surface [44], and to changes in the electrochemical responses of inert electrodes depending on their pretreatment (see, e.g. [18, 45]). Much attention has been paid to the problem of the distribution of the steady-state nucleation rate around a growing cluster of the new phase as well (see, *e.g.* [46] and Refs. cited therein).

The concept proposed in our work will be considered for inhomogeneity of polycrystalline Pt surface which may be of macroscopic rather than of microscopic or atomic range when it comes to the separate zones. To our mind, it can elucidate additionally the role of the state of the surface of an inert electrode in the nucleation-growth processes. As far as we know, such an approach has not been dealt with in the literature up to now. The proposed concept can be illustrated as follows.

The progressive 3D nucleation with a diffusion-controlled growth mechanism for Bi deposition onto the working Pt electrode is further assumed to be the case as stated above. Then, for simplicity sake, one can assume that there are two zones 1 and 2 on the surface of the Pt electrode with different values of the Bi nucleation rate, and that, say, $(aN_o)_1 > (aN_o)_2$. In terms of the theory of Scharifker and Hills [10], the nucleation rate for zone 1, $(aN_o)_1$, can be estimated from t_{max} (as from the parameter independent of the area of the electrode) using Eq.(7) and the value of D for Bi^{3+} ion taken here as $6.7 \cdot 10^{-6}$ cm^2s^{-1}. This parameter was found to be equal to $1.55 \cdot 10^{-6}$ $cm^{-2}s^{-1}$ at the particular value of η_c of 0.053 V. Then, the theoretical value of $i_{max,1}$ was calculated from Eq.(8), and $\theta_1 = i_{max,exp} / i_{max,1,calc}$ was estimated ($\theta_1 \approx 0.039$). This value of θ_1 was introduced into Eq.(3), and the current transient related only to the zone 1 was calculated (Fig. 3, curve 1). The subtraction of the calculated current transient $(i/t)_1$ from the experimental one (Fig. 3, triangles) led to the current shown by open circles. The latter data in turn, were used to determine the induction time t_{ind}, as shown in Fig. 4, and thereafter the values of $t_{max,2}$. Again, from the values of $t_{max,2}$ and D for Bi^{3+} ion, the product $(aN_o)_2$ for zone 2 can be calculated through Eq.(7). The theoretical value of $i_{max,2}$ was calculated from Eq.(8) and then θ_2 as a ratio between i_{max} denoted by open circle in Fig. 3 and $i_{max,2,calc}$ was estimated ($\theta_2 \approx 0.047$ at η_c = = 0.053 V). Analogously to the previous case, the current transient $(i/t)_2$ for zone 2 was constructed using θ_2 and Eq.(3) (Fig. 3, curve 2). Finally, summing the both calculated current transients, $(i/t)_1$ and $(i/t)_2$, the predicted total current transient was obtained (Fig. 3, entire curve 3). As can be seen, there is a good agreement between the experimental (triangles) and calculated (entire line 3) chronoamperometric data, provided the appropriate values of such parameters as aN_o and θ are applied for calculation.

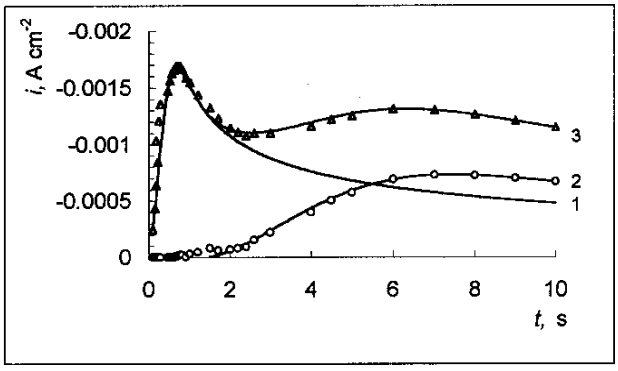

Fig. 3. Experimental (triangles taken from Fig. 1, curve 2) and calculated (full curves 1–3) current transients for η_c = 0.053 V. Open circles denote the current obtained by subtraction of the calculated curve 1 from the experimental one (triangles). Calculated curves: *1* – using $(aN_o)_1$ and θ_1 by Eq.(3), *2* – using $(aN_o)_2$ and θ_2 by Eq.(3), *3* – corresponds to a sum of curves *1* and *2*

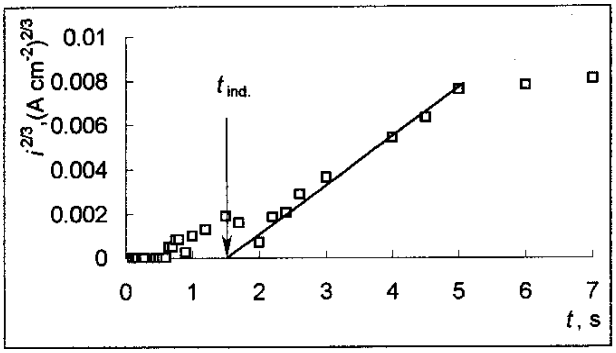

Fig. 4. $i^{2/3}$ *vs.* t curve at η_c = 0.053 V for illustration of induction time determination

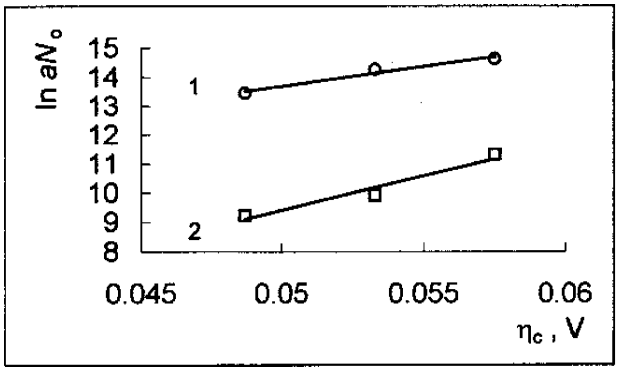

Fig. 5. Variation of the nucleation rate with overpotential for separate zones 1 (line *1*) and 2 (line *2*)

The procedure described thus far should be applied to all current transients within the η_c interval used.

As is customary, the critical number of atoms in the stable nuclei ($N_{crit.}$) can be estimated from the ln (aN_o) *vs.* η_c plot [2]:

$$N_{crit} = (RT/zF)\ [\mathrm{d}\ \ln(aN_o)/\mathrm{d}\ \eta_c]. \qquad (10)$$

Such calculated plots for zones 1 and 2 are presented in Fig. 5. From the respective slopes, it follows that $N_{crit,1}$ = 1.13 and $N_{crit,2}$ = 1.97. Rounding off these numerical quantities to the nearest whole numbers one obtain, respectively, $N_{crit,1}$ = 1 and $N_{crit,2}$ = 2. So, it can be seen, that, in the case of the zone 1, each Bi atom deposited onto the Pt electrode may be considered as a separate stable nucleous.

For the model outlined above, the θ *vs.* η_c plots were constructed for zones 1 and 2 (Fig. 6). Although the fractional surface of zone 1, θ_1, increases with η_c in the interval 0.049 to 0.057 V, its value does remain rather small. On the contrary, the analogous fractional surface relative to the zone 2, θ_2, decreases within the same interval of η_c, but this parameter is also rather small. It should be noted that the sum of θ_1 and θ_2 tends to be almost constant (Fig. 6). This finding seems to suggest that an increase in θ_1 with η_c takes place actually only at the expense of θ_2, and the total surface area of Pt accessible for Bi nucleation remains approximately constant and does not exceed 10% of the geometric surface area of the electrode. The rest of the surface of Pt electrode, therefore, can be considered as unfavourable for nucleation.

The density of nuclei at saturation, N_s, observed at long times, *i.e.* after the entire surface becomes covered with nucleation exclusion zones, is given by [10]:

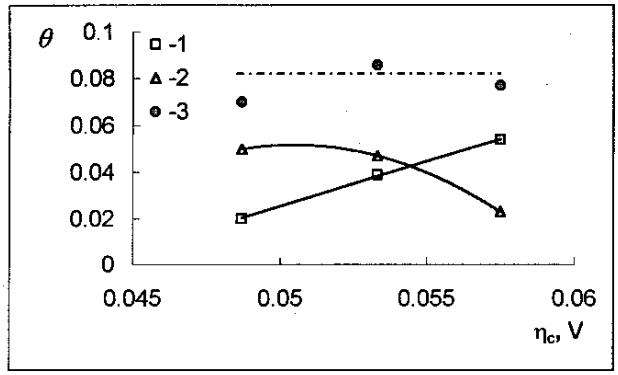

Fig. 6. Variation of fractional Pt electrode surface areas – zone 1 (*1*) and zone 2 (*2*) – and of sum of these zones (*3*) with overpotential

$$N_s = (aN_o/2k'D)^{0.5}. \qquad (11)$$

Since k' = 0.3078, as calculated from Eq.(4), D = = 6.7·10^{-6} cm^2 s^{-1} for Bi^{3+} ion, $(aN_o)_1$ = 1.55·10^6 cm^{-2} and $(aN_o)_2$ = 2·10^4 cm^{-2} at η_c = 0.053 V for zones 1 and 2, respectively, the calculation yields $N_{s,1}$ = 6.1·10^5 and $N_{s,2} \approx 7\cdot10^4$ cm^{-2}.

The parameters of Bi nucleation onto the polycrystalline Pt electrode, calculated for other values of η_c in the framework of the proposed model, are presented in Table.

Table. **Some characteristics of initial stages of Bi deposition onto smooth polycrystalline Pt from acidic 0.1 M Bi^{3+} perchlorate solution, taking into account the presence of separate zones with different nucleation rates on the surface of the working electrode**

Overpotential, mV	Zone 1			Zone 2		
	θ_1	$(aN_o)_1$, cm^{-2}s^{-1}	$N_{s,1}$, cm^{-2}	θ_2	$(aN_o)_2$, cm^{-2}s^{-1}	$N_{s,2}$, cm^{-2}
49	0.0200	8.00 ·10^5	4.41 ·10^5	0.050	7.20 ·10^3	4.18 ·10^4
53	0.0387	1.55 ·10^6	6.14 ·10^5	0.047	2.00 ·10^4	6.97 ·10^4
57	0.0540	2.23 ·10^6	7.36 ·10^5	0.023	8.00 ·10^4	1.39 ·10^5

To conclude, it was shown that the current transients observed at Bi electrocrystallization onto polycrystalline Pt within a certain range of overpotentials can be described by a model involving the presence of separate surface zones with different metal nucleation rates. It was also shown that the initial stages of Bi deposition onto polycrystalline smooth Pt from acidic perchlorate solution can be described by the progressive 3D nucleation and diffusion-controlled growth mechanism [10], taking into account the presence of the aforementioned separate surface zones.

CONCLUSIONS

When investigating the initial stages of Bi deposition onto a polycrystalline smooth Pt electrode from acidic perchlorate solution, it was found that the potentiostatic current transients recorded within a certain range of overpotentials can be described by the model involving progressive 3D nucleation and diffusion-controlled growth mechanism [10], taking into account the presence of separate surface zones with different Bi nucleation rates. These surface zones should be of macroscopic dimensions rather than microscopic or atomic ones.

Received 2
October 2000
Accepted
30 October 2000

References

1. G. A. Somorjai, *Introduction to Surface Chemistry and Catalysis,* John Wiley & Sons, Inc., New York–Chichester–Brisbane–-Toronto–Singapore (1994).
2. E. Budevski, G. Staikov, and W. J. Lorenz, *Electrochemical Phase Formation and Growth,* VCH, Weinheim–New York–Basel–Cambridge–Tokyo (1996).
3. Yu. D. Gamburg, *Electrochemical Crystallization of Metals and Alloys,* Yanus-K, Moscow (1997) (in Russian).
4. E. Budevski, G. Staikov, and W. J. Lorenz, *Electrochim. Acta,* **45**, 2559 (2000).
5. M. Fleischmann and H. R. Thirsk, in *Advances in Electrochemistry and Electrochemical Engineering,* Vol. 3 (Ed. P. Delahay), Ch. 3, Interscience Publishers, New York–London (1963).
6. A. Milchev, S. Stoyanov and R. Kaischev, *Thin Solid Films,* **22**, 255 (1974).
7. G. Gunawardena, G. Hills, I. Montenegro and B. Scharifker, *J. Electroanal. Chem.* **138**, 225 (1982).
8. E. Budevski, in *Comprehensive Treatise of Electrochemistry*, Vol. 7 (Eds. B. E. Conway, J. O'M. Bockris, E. Yeager, S. U. M. Khan and R. E. White), Ch. 7 (Part A), Plenum Press, New York-London (1983).
9. S. Fletcher, *Electrochim. Acta,* **28**, 917 (1983).
10. B. Scharifker and G. Hills, *Electrochim. Acta*, **28**, 879 (1983).
11. B. R. Scharifker and J. Mostany, *J. Electroanal. Chem.*, **177**, 13 (1984).
12. V. Tsakova and A. Milchev, *J. Electroanal. Chem.*, **235**, 237 (1987).
13. W. S. Kruijt, M. Sluyters-Rehbach, J. H. Sluyters and A. Milchev, *J. Electroanal. Chem.*, **371**, 13 (1994).
14. B. Bhattacharjee and S. K. Rangarajan, *J. Electroanal. Chem.*, **366**, 271 (1994).
15. A. Kelaidopoulou, G. Kokkinidis and A. Milchev, *J. Electroanal. Chem.*, **444**, 195 (1998).
16. L. Heerman and A. Tarallo, *J. Electroanal. Chem.*, **470**, 70 (1999).
17. A. Milchev, *Electrochim. Acta*, **28**, 947 (1983).
18. H. Bort, K. Jüttner, W. J. Lorenz, G. Staikov and E. Budevski, *Electrochim. Acta*, **28**, 985 (1983).
19. R. R. Adžić, in *Advances* in *Electrochemistry and Electrochemical Engineering,* Vol. 11 (Eds. H. Gerischer and Ch. W. Tobias), p. 159, John Wiley & Sons, New-York-Chichester-Brisbane-Toronto-Singapore (1984).
20. G. Kokkinidis, *J. Electroanal. Chem.*, **201**, 217 (1986).
21. K. Jüttner, *Electrochim. Acta*, **31**, 917 (1986).
22. B. J. Bowles, *Electrochim. Acta*, **15**, 737 (1970).
23. F. Mikuni and T. Takamura, *Denki Kagaku*, **39**, 579 (1971).
24. S. H. Cadle and St. Bruckenstein, *Anal. Chem*., **44**, 1993 (1972).
25. R. R. Adžić, D. N. Simić, A. R. Despić, and D. M. Dražić, *J. Electroanal. Chem.*, **65**, 587 (1975).
26. S. Szabo and F. Nagy, *J. Electroanal. Chem.*, **70**, 357 (1976).
27. N. Furuya and S. Motoo, *J. Electroanal. Chem.*, **98**, 189 (1979).
28. I. Fonseca, J. Lin-Cai and D. Pletcher, *J. Electroanal. Chem.*, **130**, 2187 (1983).
29. R. R. Adžić and N. N. Marković, *Electrochim. Acta,* **30**, 1473 (1985).
30. J. Clavilier, J. M. Feliu and A.Aldaz, *J. Electroanal. Chem.*, **243**, 419 (1988).
31. J. Clavilier, J. M. Feliu, A. Fernandez-Vega and A. Aldaz, *J. Electroanal. Chem.*, **269**, 175 (1989).
32. R. Gómez, A. Fernandez-Vega, J. M. Feliu and A. Aldaz, *J. Phys. Chem.*, **97**, 4769 (1993).
33. M. R. Evans and G. A. Attard, *J. Electroanal. Chem.*, **345**, 337 (1993).
34. C. P. Wilde and M. Zhang, *Langmuir*, **10**, 1600 (1994).
35. G. Salié and K. Bartels, *Electrochim. Acta,* **39**, 1057 (1994).
36. W.-F. Lin, S.-G. Sun and Z.-W. Tian, *J. Electroanal. Chem.*, **364**, 1 (1994).
37. R. Gómez, J. M. Feliu and A. Aldaz, *Electrochim. Acta,* **42**, 1675 (1997).
38. U. W. Hamm, D. Kramer, R. S. Zhai and D. M. Kolb, *Electrochim. Acta,* **43**, 2969 (1998).
39. A. Steponavičius and L. Gudavičiūtė, *Chemija (Vilnius)* (in press).
40. A. Steponavičius, L. Gudavičiūtė, V. Karpavičienė and V. Kapočius, *Chemija (Vilnius)* (in press).
41. T. Biegler, D. A. J. Rand, and R. Woods, *J. Electroanal. Chem.*, **29**, 269 (1971).

42. H. Angerstein-Kozlowska, B.E. Conway, and W. B. A. Sharp, *J. Electroanal. Chem.*, **43**, 9 (1973).
43. H. Angerstein-Kozlowska, B. E. Conway, B. Barnett and J. Mozota, *J. Electroanal. Chem.*, **100**, 417 (1979).
44. R. L. Deutscher and S. Fletcher, *J. Electroanal. Chem.*, **239**, 17 (1988).
45. M. H. Hölzle, V. Zwing and D. M. Kolb, *Electrochim. Acta,* **40**, 1237 (1995).
46. A. Milchev, W. S. Kruijt, M. Sluyters-Rehbach, and J. H. Sluyters, *J. Electroanal. Chem.*, **362**, 21 (1993).

V. Kapočius, L. Gudavičiūtė, V. Karpavičienė, A. Steponavičius

POLIKRISTALINIO PLATINOS ELEKTRODO SU SKIRTINGAIS BRANDUOLIŲ UŽUOMAZGŲ SUSIDARYMO GREIČIAIS ĮVAIRIOSE PAVIRŠIAUS ZONOSE MODELIO TAIKYMAS APRAŠANT BISMUTO NUSODINIMO PRADINES STADIJAS PERCHLORATINIAME TIRPALE

S a n t r a u k a

Bi nusodinimo ant glotnaus polikristalinio Pt elektrodo pirmosios stadijos rūgščiame 0,1 M Bi^{3+} perchloratiniame tirpale esant 20°C temperatūrai buvo tiriamos taikant potencialo įjungimo metodą. Remiantis potenciostatinių „srovė–laikas“ priklausomybių analize, parodyta, kad Bi elektrokristalizacijos ant Pt pirmosios stadijos pakankamai gerai aprašomos Scharifker ir Hills progresuojančio 3D branduolių užuomazgų susidarymo ir difuzijos kontroliuojamo augimo mechanizmu atsižvelgiant į atskiras su skirtingais branduolių užuomazgų susidarymo greičiais zonas elektrodo paviršiuje. Taip pat padaryta prielaida, kad šios atskiros zonos gali būti greičiau makroskopinių dydžių eilės negu mikroskopinių ar atominių.

В. Капочюс, Л. Гудавичюте, В. Карпавичене, А. Степонавичюс

МОДЕЛЬ ПОЛИКРИСТАЛЛИЧЕСКОГО ПЛАТИНОВОГО ЭЛЕКТРОДА С НЕОДИНАКОВОЙ СКОРОСТЬЮ ЗАРОДЫШЕОБРАЗОВАНИЯ В РАЗНЫХ ЗОНАХ ПОВЕРХНОСТИ ДЛЯ ОПИСАНИЯ НАЧАЛЬНЫХ СТАДИЙ ОСАЖДЕНИЯ БИСМУТА В ПЕРХЛОРАТНОМ РАСТВОРЕ

Р е з ю м е

Начальные стадии осаждения Bi на гладком поликристаллическом Pt электроде в кислом 0,1 M Bi^{3+} перхлоратном растворе при температуре 20°C исследовали с применением метода потенциостатического включения. На основе анализа потенциостатических зависимостей „ток–время“ показано, что начальные стадии электрокристаллизации Bi на Pt довольно хорошо описываются механизмом 3D зародышеобразования и диффузией контролируемого роста, предложенным Шарифкером и Хиллсом, с учетом присутствия на поверхности электрода отдельных зон с неодинаковой скоростью зародышеобразования. Высказано также предположение, что эти зоны имеют скорее макроскопические размеры, чем микроскопические или атомные.